THE JOURNAL OF PHYSICAL CHEMISTRY B

pubs.acs.org/JPCB Article

Electrodeposition of ZnNi Alloys from Choline Chloride/Ethylene Glycol Deep Eutectic Solvent and Pure Ethylene Glycol for Corrosion Protection

Published as part of The Journal of Physical Chemistry virtual special issue "Deep Eutectic Solvents".

R. Bernasconi, G. Panzeri, G. Firtin, B. Kahyaoglu, L. Nobili, and L. Magagnin*

Cite This: *J. Phys. Chem. B* 2020, 124, 10739−10751 Read Online

ACCESS | Metrics & More | Article Recommendations | Supporting Information

ABSTRACT: The present work follows the trend to develop nonaqueous electrolytes for the deposition of corrosion resistant ZnNi alloys. It investigates the use of the choline chloride/ethylene glycol (1:2 molar ratio) eutectic mixture and of pure ethylene glycol as solvents for ZnNi electroplating. The electrochemical behavior of Zn and Ni is investigated via cyclic voltammetry, and potentiostatic ZnNi deposition is performed. Ni content is found to be precisely tunable in the 10−20% wt range, which presents the highest industrial interest for corrosion protection. ZnNi coatings obtained are characterized from the morphological and phase composition point of view. Evidence of the formation of a metastable γ ZnNi phase is observed for both choline chloride/ethylene glycol and pure ethylene glycol. Finally, potentiodynamic corrosion tests are performed to assess their corrosion properties.

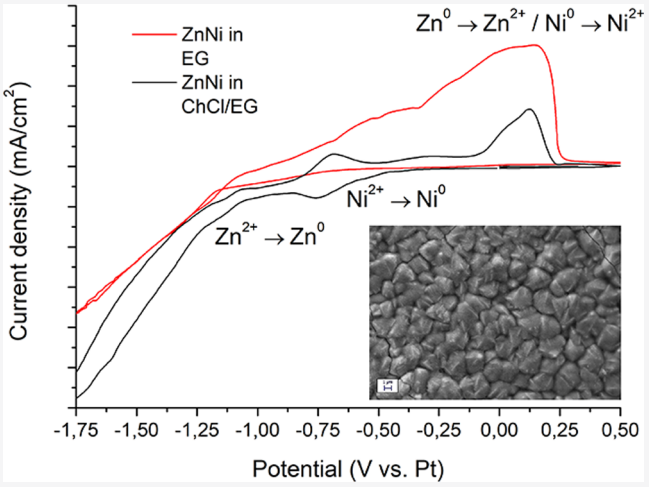

INTRODUCTION

Electrodeposited zinc−nickel alloys are widely employed in surface finishing as corrosion protection coatings on steel substrates.[1,2] Among the possible film compositions, zinc-rich stoichiometry is one of the most exploited due to the low corrosion potential of the γ-phase (9−15% wt Ni) that makes it an ideal sacrificial layer in case the substrate is exposed to the environment.[2] Aside from being largely used at the industrial level, the scientific community investigated the ZnNi system also because it undergoes anomalous co-deposition,[3] where the less noble element is preferentially deposited under the majority of plating conditions regardless of the relative ionic concentration in the plating bath.[4,5] This poses a limitation, since the corrosion properties of the coating are difficult to be tailored if relying on aqueous systems, due to the poor control on composition. The increase in nickel content would indeed lower the driving force of the galvanic couple but would increase the lifetime of the coating itself due to the lower corrosion rate.[6]

For these reasons, organic solutions were considered as a possible substitute for the traditional aqueous ones, showing higher control on the alloy composition.[7−11] In the framework of nonaqueous solutions, choline chloride based deep eutectic solvents (DESs)[12] are one of the most investigated systems alternatively to traditional plating,[13−15] counting several efforts toward making them appealing for industrial applications.[16−24] Their relative low cost, sustainability, and physicochemical properties have indeed attracted the attention of researchers aiming to improve the coating properties and/or the process efficiency with respect to water based ones, as in the case of Zn[25−31] and Zn based alloys.[32−38] The wider electrochemical window of these DESs (2.1−2.2 V for choline chloride/urea 1:2 mixtures; 1.7−2.1 V for choline chloride/ethylene glycol 1:2 mixtures[39]) makes them suitable for the plating of metals with low reduction potential by limiting the onset of secondary reactions such as hydrogen evolution, affecting both coating and substrate properties.[40−42] In turn, DESs are also characterized by significant drawbacks. In particular, their comparatively high viscosity reduces mass transfer of electro-

Received: May 27, 2020
Revised: October 30, 2020
Published: November 11, 2020

https://dx.doi.org/10.1021/acs.jpcb.0c04784
J. Phys. Chem. B 2020, 124, 10739−10751

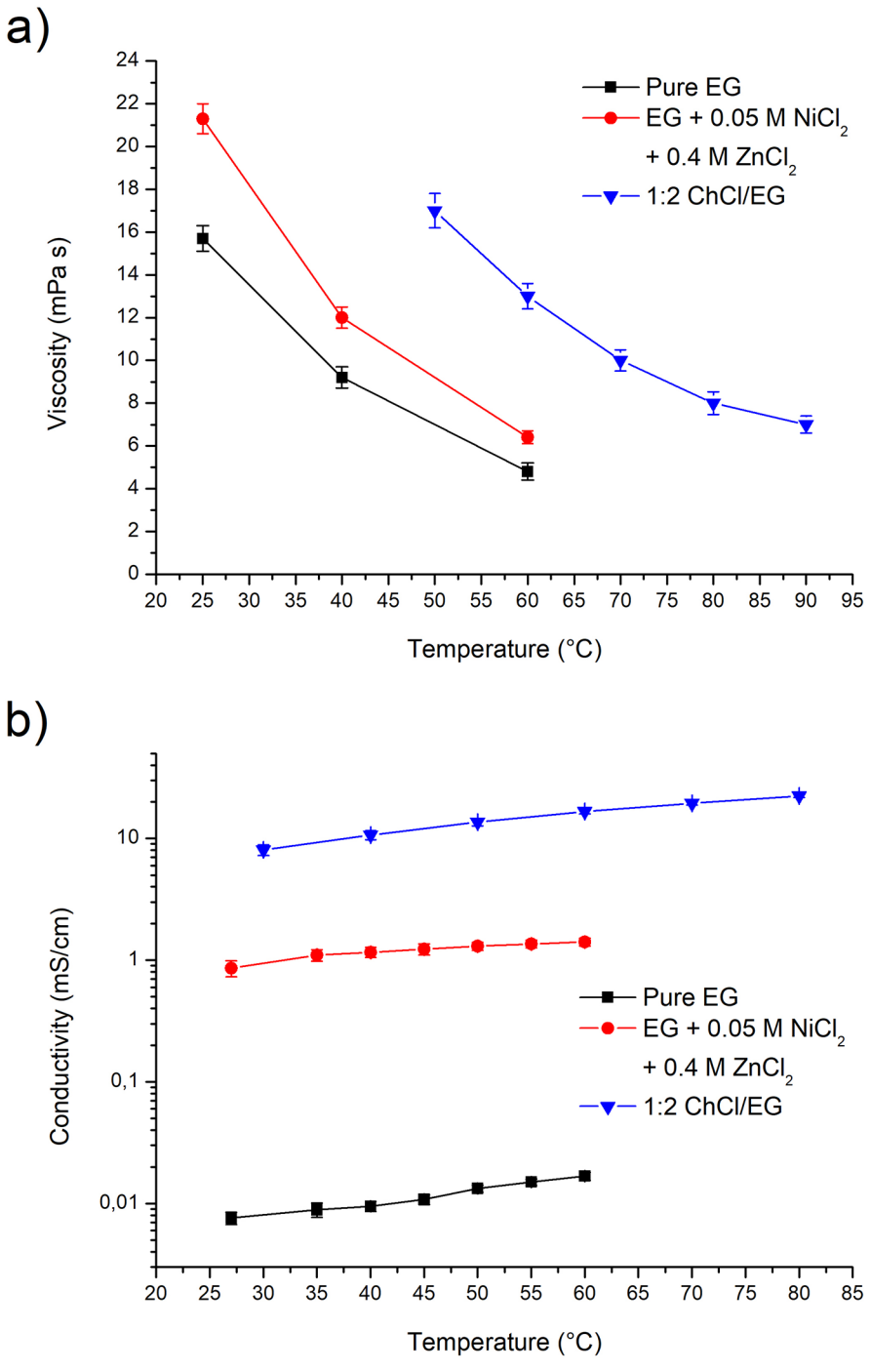

Figure 1. Viscosity vs temperature (a) and conductivity vs temperature (b) graphs for ChCl/EG 1:2, pure EG, and pure EG + 0.4 M $ZnCl_2$ and 0.05 M $NiCl_2$.

active species.[43] Moreover, the purity of the DES components is harder to control with respect to aqueous solutions.

The electrodeposition of Zn−Ni alloys, in the framework of DES, has been investigated mostly from the choline chloride/urea system (1ChCl:2U).[7,9−11] The study of Yang et al.[7] focused on the synthesis and characterization of Ni-rich alloys (50−100 % wt Ni). The zinc content progressively increased with the cathodic potential applied, associated with the formation of cracks in the film. Fashu et al.[9,10] further examined this system by exploring the effect of the different experimental parameters and additives (EDTA and NH_4Cl) aiming at the formation of a smooth and crack-free Ni-rich film. Conversely, Zn-rich coatings were obtained by tailoring the water content in the 1ChCl:2U solution, shifting the compositional window from 50−100% wt to 5−40% wt of nickel.[11] The corrosion properties of the coating were investigated at different compositions, showing higher corrosion potentials and lower corrosion currents progressively increasing the nickel content. Ethylene glycol based DES (1ChCl:2EG), on the other hand, was first investigated for the ZnNi alloy electrodeposition by Pereira et al.,[8] focusing on the effect of amines on the morphology of zinc-rich films having 5−7% wt Ni. The system was allowed to cover a broader

https://dx.doi.org/10.1021/acs.jpcb.0c04784
J. Phys. Chem. B 2020, 124, 10739−10751

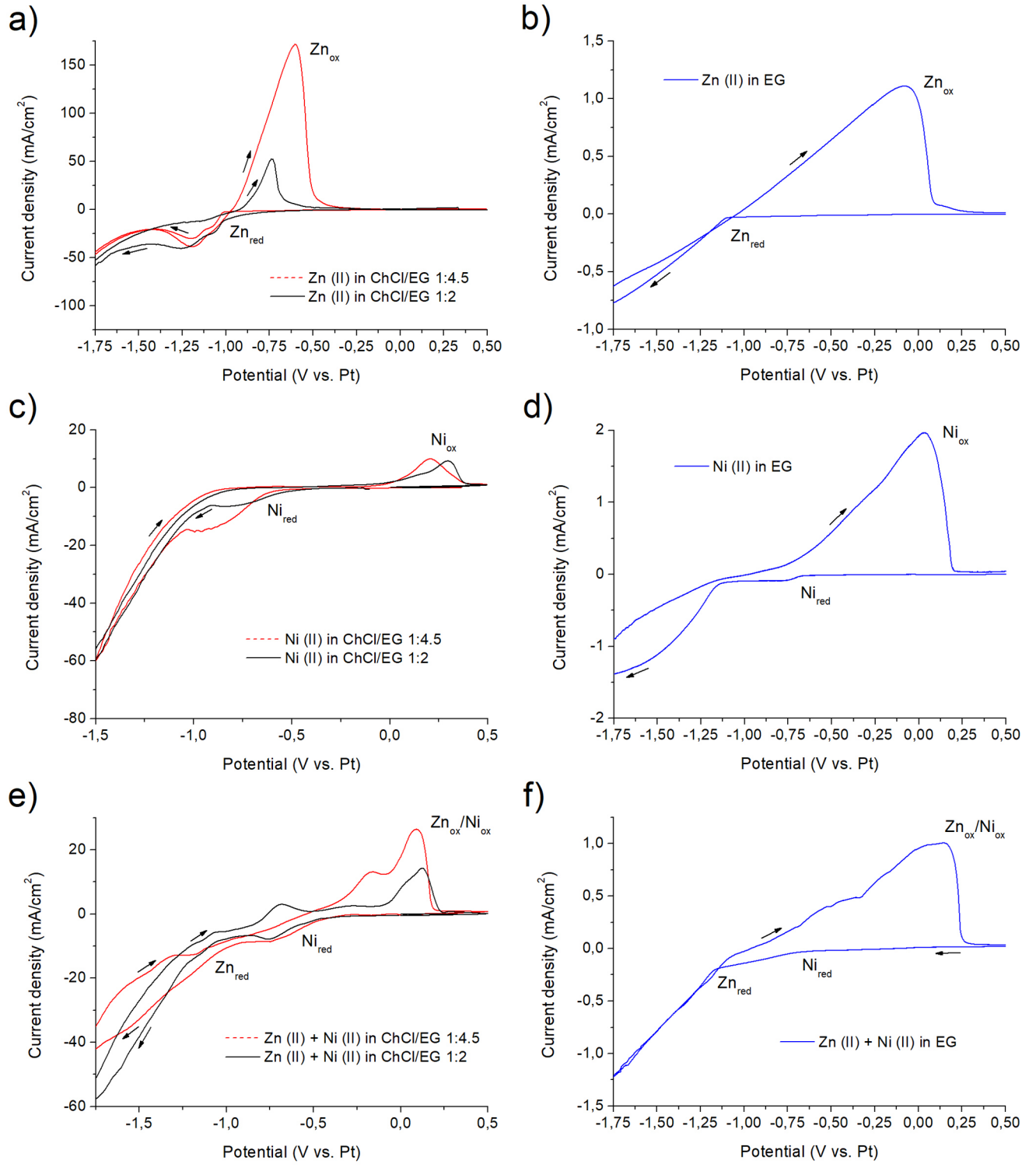

Figure 2. Cyclic voltammetries for different electrolytes: ChCl/EG + Zn (a), EG + Zn (b), ChCl/EG + Ni (c), EG + Ni (d), ChCl/EG + Zn + Ni (e), EG + Zn + Ni (f).

compositional window (3−80% wt Ni),[44] at a fixed electrolyte composition, with respect to the urea based one.

Literature studies also reported the possibility to use bare ethylene glycol (EG) as a solvent, avoiding or limiting the chloride concentration in the bath,[45−52] showing beneficial effects on coating properties[53] and affecting the electrochemical behavior of the cationic species.[54] Although the chloride ions coming from choline chloride (ChCl) are responsible for the relatively high conductivity value of these electrolytes, they may affect the electrodeposit because of their intrinsic aggressivity, especially in the case of low nobility metals or alloys, such as zinc-rich ones.

In this work, we studied the effect of choline chloride concentration on the co-electrodeposition of ZnNi alloys with

https://dx.doi.org/10.1021/acs.jpcb.0c04784
J. Phys. Chem. B 2020, 124, 10739−10751

the focus on how anomalous deposition is affected. The well-known deep eutectic solvent choline chloride/ethylene glycol (ChCh/EG in 1:2 molar ratio) is compared to a plating bath relying only on ethylene glycol as solvent. Electrolytes' physical and electrochemical properties are investigated, and potentiostatic deposition on iron substrates is performed. Resulting ZnNi coatings are then characterized from the morphological point of view, and their phase composition is determined. Finally, corrosion protection performances of the ZnNi layers obtained from ChCl/EG 1:2 and EG are determined.

METHODS

Anhydrous ethylene glycol ($C_2H_6O_2$; Sigma-Aldrich; purity 99.8%; water content ≤0.003%), choline chloride ($C_5H_{14}ClNO$; Sigma-Aldrich; purity ≥99%; water content ≤0.5%), zinc(II) chloride ($ZnCl_2$; Sigma-Aldrich; purity ≥98%), and nickel(II) chloride hexahydrate ($NiCl_2{\cdot}6H_2O$; Sigma-Aldrich; purity ≥98%) were used as received. Three base solvents were employed: a ChCl/EG 1:2 molar ratio mixture, a ChCl/EG 1:4.5 molar ratio mixture, and pure EG. Ni and Zn salts were dissolved in these three solvents according to the quantities detailed in the results part, and the resulting electrolytes were used to perform ZnNi deposition. Solutions were maintained at the usage temperature (70 °C for ChCl/EG 1:2 and ChCl/EG 1:4.5 based baths; 60 °C for pure EG based baths) during solution preparation, electrochemical characterization, and electrodeposition using a thermal jacket controlled by a thermocouple. Where specified, samples were annealed at 400 °C for 1 h in an inert atmosphere (N_2). The electrochemical characterization was performed in a standard three-electrode cell setup, employing an AMEL2550 potentiostat/galvanostat. Cyclic voltammetry (CV) was done using a platinum wire as working, counter, and reference electrodes. A 20 mV/s scan rate was employed, and no stirring was applied. An AMEL2550 potentiostat/galvanostat was used also to perform potentiostatic deposition tests. In this case, however, mild steel plates were used as working electrodes, while a platinum wire was used as reference and counter electrode. The steel surface was cleaned in acetone and etched in a 20% wt HCl solution to remove surface oxides. Cathodic efficiencies in the 60−70% range were observed for Ni contents ranging from 16 to 18% wt. Potentiodynamic polarization tests were done in a 5% wt NaCl aqueous solution. A 1 mV/s scan rate was employed, and the solution was not stirred. SEM was carried out employing a Zeiss EVO 50 EP setup, equipped with an energy dispersive spectroscopy (EDS) module (Oxford instruments INCA). A Philips PW1830 ($K_{\alpha 1Cu}$ = 1.54058 Å) setup was employed to perform XRD. Film composition was determined by X-ray fluorescence spectroscopy (XRF), using a Fischerscope X-ray XAN. Conductivity was measured using a AMEL model 2131 conductivity meter, while viscosity was evaluated using a Haake Viscotester VT5R rotational viscometer. Electrolyte water content was determined via Karl Fischer titration with a Metrohm 870 KF Titrino Plus. Both deposition experiments and characterization tests were repeated at least twice to evaluate repeatability. No significant deviations from the data presented were observed.

RESULTS AND DISCUSSION

Electrolyte Water Content. Water content is an important parameter in the case of electrodeposition from nonaqueous solutions, since it considerably influences the electrochemical behavior of the metallic ions present in the bath, the potential window of the electrolyte, and its conductivity/viscosity. In the case of deep eutectic solvents, water contamination can be beneficial or detrimental according to the metal plated. For example, Ni electrodeposition in 1:2 choline chloride−urea is negatively affected by water concentrations higher than 4.5% wt. Under these conditions, as demonstrated by Lukaczynska et al.,[55] the Ni coating incorporates degradation products from the electrolyte. On the other side, Cu deposition in 1:2 ChCl/EG is positively affected by water. Valverde et al.[56] demonstrated that water increases deposition rates and electrolyte conductivity.

Table 1. E_{on} Values for the Voltammetries Depicted in Figure 2

solvent	E_{on} Zn_{red} in Zn bath	E_{on} Ni_{red} in Ni bath	E_{on} Zn_{red} in ZnNi bath	E_{on} Ni_{red} in ZnNi bath	ΔE_{on} Zn_{red}/Ni_{red} in ZnNi
ChCl/EG 1:2	−1.01	−0.52	−1.17	−0.5	0.67
ChCl/EG 1:4.5	−1.02	−0.62	−1.07	−0.55	0.52
pure EG	−1.11	−0.67	−1.17	−0.68	0.49

In front of these considerations, the water concentration of the electrolytes employed in the present work was estimated. By considering only the water content declared by the manufacturer for the solvents employed (ChCl/EG and pure EG), water concentration was limited to less than 0.003% wt in the case of pure EG, 0.169% wt for ChCl/EG 1:4.5, and 0.266 wt % in the case of ChCl/EG 1:2. However, additional water was incorporated from the nickel salt employed, which was hydrated. To quantify water content, Karl Fischer titration was performed on the electrolytes with the highest expected water content. These are the ones containing the highest concentration of nickel chloride: ChCl/EG + 0.2 M $ZnCl_2$ + 0.13 M $NiCl_2$ and EG + 0.2 M $ZnCl_2$ + 0.15 M $NiCl_2$. The results obtained evidenced a water content equal to 1.54 ± 0.02% wt for the ChCl/EG based electrolytes and to 1.42 ± 0.02% wt in the case of the electrolyte based on EG.

It is fundamental to emphasize, however, that the electrolytes change their water content with time due to atmospheric moisture absorption. Indeed, both ChCl and EG are hygroscopic. This contribution is hard to quantify, as it depends on the temperature of the solution, the relative humidity of the air and the exposure time to humidity itself. It has been reported in the literature[57] that maintaining the solution at high temperature significantly limits water uptake. As an example, ChCl/EG at room temperature rapidly incorporates water and reaches a content equal to 40% wt after 60 days. If the same solution is heated at 80 °C, the water content decreases to 1.5% wt after 18 days.

Electrolyte Physical Properties. The general physical behavior of ChCl/EG 1:2 based electrolytes is relatively well-known.[58] The same is true for non-eutectic mixtures of ChCl/EG (like the 1:4.5 molar ratio[59]) but not for pure EG based electrolytes, since they have been developed only in the past few years. Therefore, it is fundamental to provide a clear characterization of their physical properties, in particular viscosity and conductivity. A very high viscosity may constitute an issue for electrodeposition, since highly viscous fluids are typically characterized by reduced ionic mobility. At the same time, a low conductivity may represent a serious obstacle for successful metal deposition, with reduced power efficiencies and difficulties in the formation of uniform layers.[60,61]

https://dx.doi.org/10.1021/acs.jpcb.0c04784
J. Phys. Chem. B 2020, 124, 10739−10751

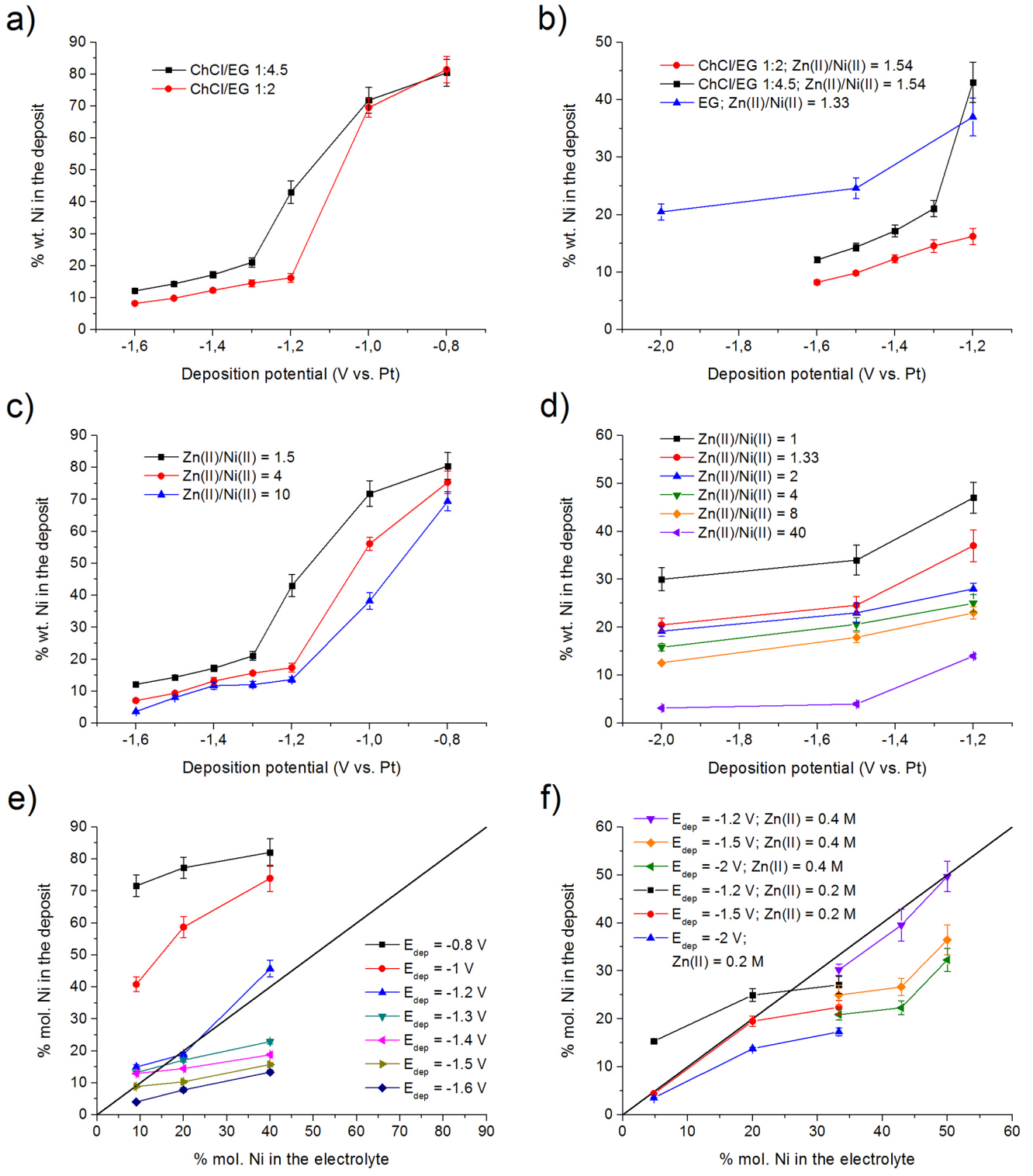

Figure 3. Effect of ChCl/EG ratio variation on Ni content as a function of deposition potential (a and b); effect of Zn(II)/Ni(II) ratio variation on Ni content as a function of deposition potential in ChCl/EG (c); effect of Zn(II)/Ni(II) ratio variation on Ni content as a function of deposition potential in EG (d); Ni % mol. in the deposit vs Ni % mol. in the bath for ChCl/EG (e); Ni % mol. in the deposit vs Ni % mol. in the bath for EG (f).

ChCl/EG 1:2 and EG dynamic viscosity was determined, and it is plotted in Figure 1a. Coherently with state-of-the-art measurements,[58] ChCl/EG 1:2 was characterized by a relatively high viscosity, which reached values suitable for electrodeposition only at rather high temperatures. This is a consequence of the ionic nature of the fluid and of the dimension of the choline anion, which is quite large and characterized by low mobility. As a result of its high viscosity, electrodeposition from ChCl/EG 1:2 is normally performed in the 70−80 °C temperature range.

https://dx.doi.org/10.1021/acs.jpcb.0c04784
J. Phys. Chem. B 2020, 124, 10739−10751

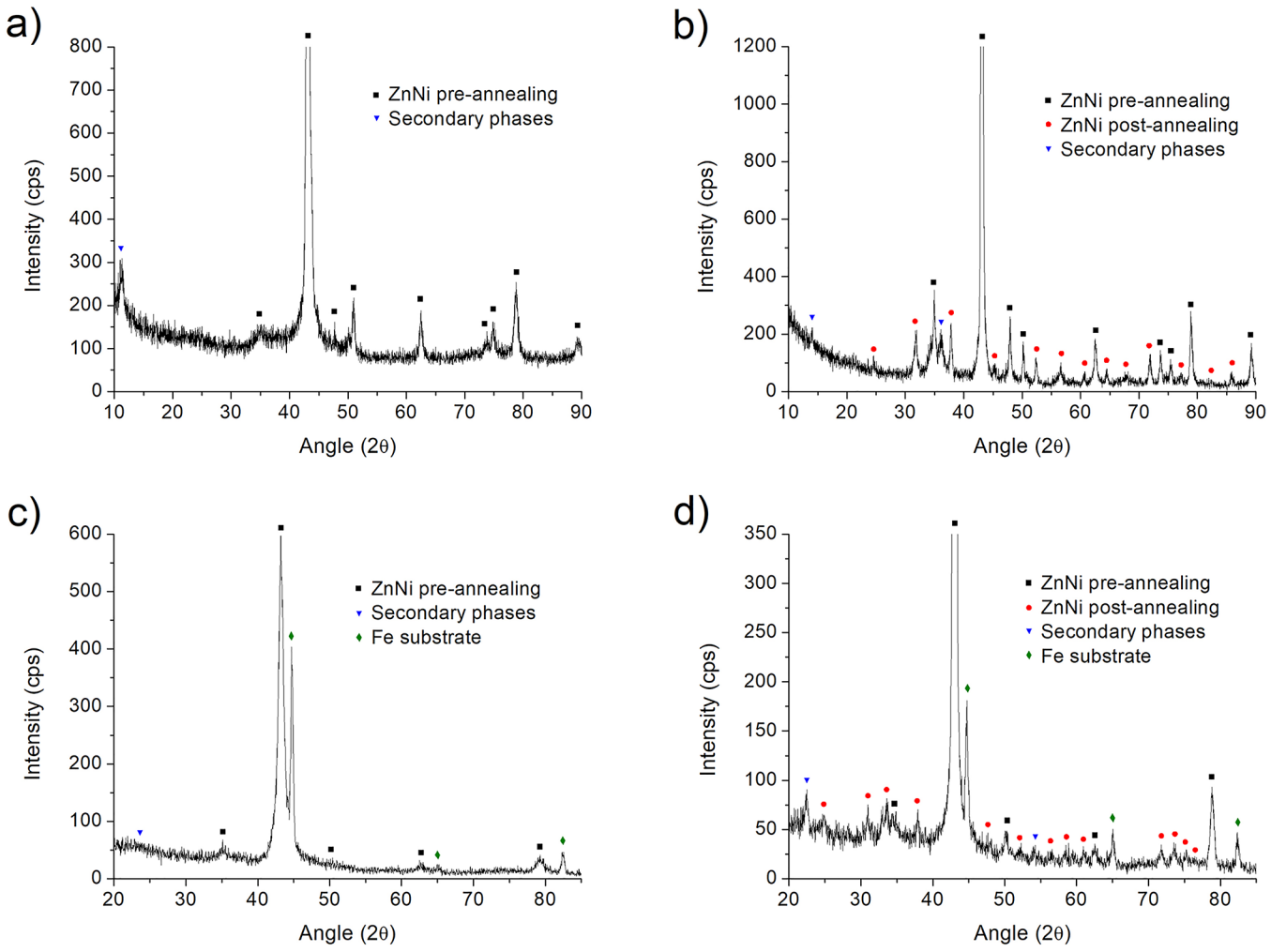

Figure 4. XRD graphs for as-plated ZnNi layers plated from ChCl/EG (a) and from EG (c); XRD graphs for annealed ZnNi layers plated from ChCl/EG (b) and from EG (d).

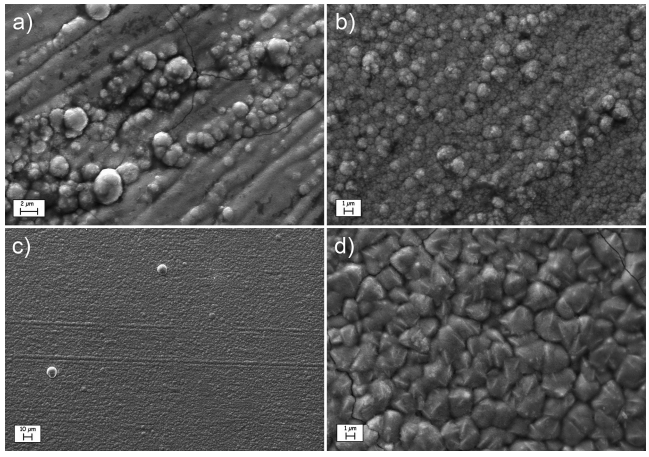

Figure 5. SEM morphology of the ZnNi layer electrodeposited from ChCl/EG 1:2 (a), ChCl/EG 1:4.5 (b), and EG (c and d). Magnification values: 10,000× (a, b, and d), 1000× (c).

Pure EG, contrarily to the ChCl/EG 1:2 mixture, is not an ionic fluid, and it presents a reduced molecular dimension with respect to choline. Consequently, its viscosity at room temperature is only 1 order of magnitude higher than water and it is roughly 4 times higher at 60 °C. As a result, electrodeposition can be potentially performed also in the 40−60 °C range. The addition of metallic salts typically affects electrolyte viscosity, and for this reason, the complete ZnNi EG based electrolyte (containing 0.4 M $ZnCl_2$ and 0.05 $MNiCl_2$) was characterized and compared to pure EG. As shown in Figure 1a, the viscosity increased by 30.4% at 60 °C, by 33.3% at 40 °C, and by 35.7% at 25 °C. All of the viscosity plots obtained follow the typical Arrhenius relationship, which exponentially correlates viscosity with temperature.[62]

As anticipated, another important property that both ChCl/EG 1:2 and EG based ZnNi electrolytes should present is a relatively high conductivity. This property is fundamental to perform efficient electrodeposition and is, for virtually all ionic liquids, linearly dependent from the reciprocal of viscosity. ChCl/EG 1:2 and EG are, however, radically different systems: ChCl/EG 1:2 is an ionic fluid presenting a high intrinsic dissociation, while EG is a non-dissociated diol. Consequently, while ChCl/EG 1:2 is well-known for its relatively high conductivity,[58] EG presents a poor conductivity (Figure 1b).

Analogously to water, however, EG readily dissolves metal salts, which can thus dissociate and provide additional conductivity. Indeed, when the ZnNi EG based electrolyte (containing 0.4 M $ZnCl_2$ and 0.05 M $NiCl_2$) was characterized, a conductivity 2 orders of magnitude higher than pure EG was observed. This indicates a high level of dissociation for metal

https://dx.doi.org/10.1021/acs.jpcb.0c04784
J. Phys. Chem. B 2020, 124, 10739−10751

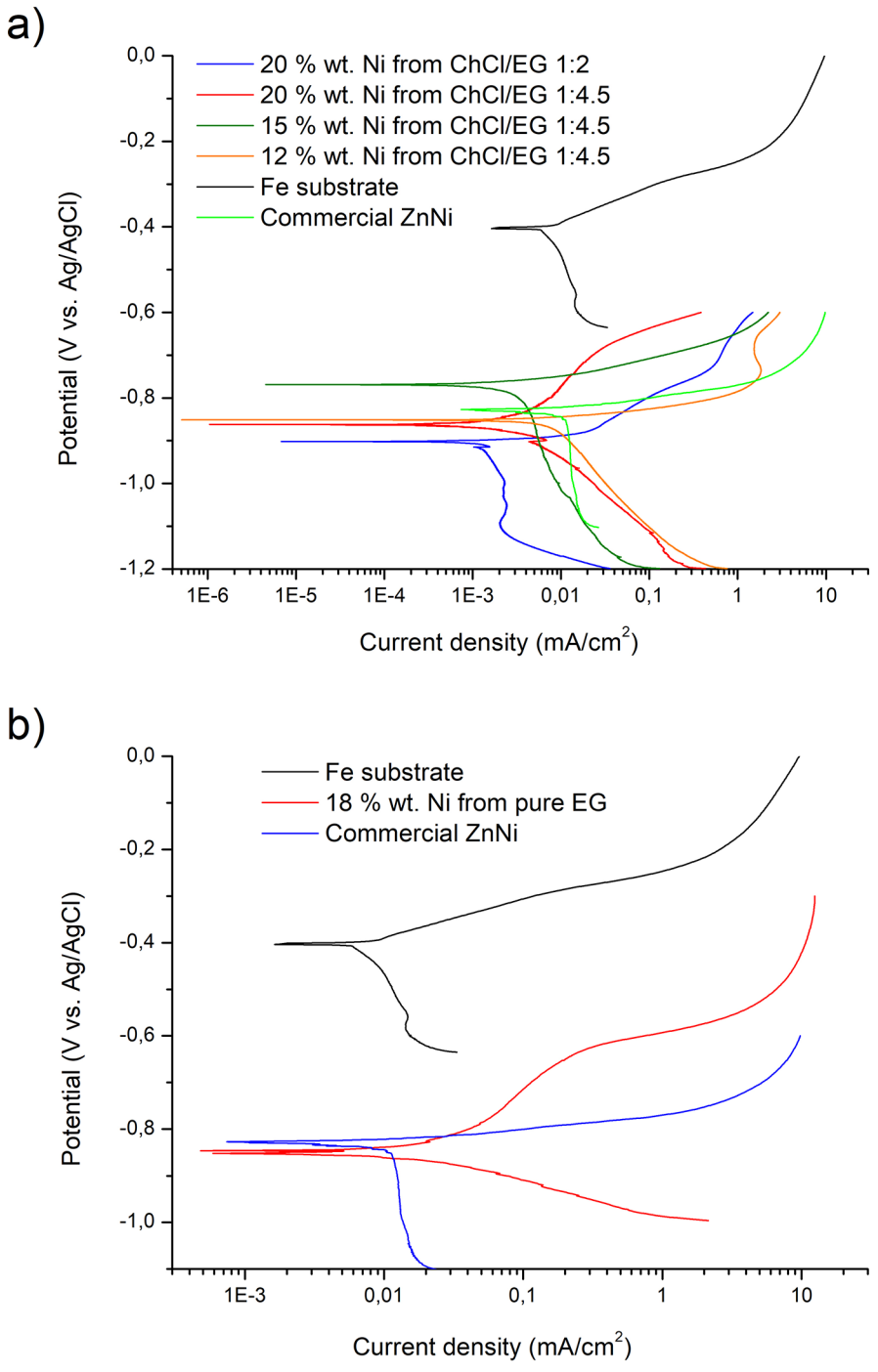

Figure 6. Potentiodynamic corrosion tests performed on ZnNi layers plated from ChCl/EG (a) and from EG (b); the corrosion behavior of the Fe substrate and of a commercial ZnNi layer is reported for comparison.

Table 2. Corrosion Data for ZnNi Alloys and Fe Substrate

sample	E_{corr} (mV vs Ag/AgCl)	I_{corr} (μA/cm^2)
Fe substrate	−402	7.5
20% Ni wt from ChCl/EG 1:2	−902	1.6
20% Ni wt from ChCl/EG 1:4.5	−859	4.3
15% Ni wt from ChCl/EG 1:4.5	−774	3.7
12% Ni wt from ChCl/EG 1:4.5	−853	7.9
18% Ni wt from pure EG	−852	18.1
15% Ni wt commercial ZnNi	−826	11.8

salts when dissolved in EG. The ZnNi EG electrolyte was characterized by a conductivity between 1.2 and 1.4 mS/cm in the 40−60 °C range, which is potentially compatible with electrodeposition.

As a result of the data obtained from the physical characterization of the different solvents, a temperature of 70 °C was selected for ChCl/EG 1:2 and a temperature of 60 °C was employed for pure EG. In the case of ChCl/EG, a temperature equal to 70 °C allowed excessive energy usage to be limited. For EG, a temperature of 60 °C resulted in optimal viscosity values.

https://dx.doi.org/10.1021/acs.jpcb.0c04784
J. Phys. Chem. B 2020, 124, 10739−10751

Electrochemical Characterization. Before performing ZnNi electrodeposition, the electrochemical behavior of the different electrolytes was investigated. The use of Pt as a pseudoreference electrode was motivated by the fact that standard reference electrodes are based on aqueous solutions, which are incompatible with DESs. This, in addition to the relatively high temperatures employed, prevented the use of standard reference electrodes. Cyclic voltammetry was performed on both ChCl/EG 1:2 and EG based ZnNi solutions. Voltammetries of ChCl/EG 1:2 and EG based baths containing only Zn or Ni were acquired to investigate the behavior of the single metallic species. Furthermore, a ChCl/EG mixture presenting an increased EG content (1:4.5 molar ratio in place of 1:2) was employed as well. In this regard, the lower concentration of ChCl, from 33 to 15−25%, would result in an increase of the ionic conductivity despite the decrease in Cl^- concentration.[59] Zn, Ni, and ZnNi electrolytes based on this solvent were characterized because they are representative of an intermediate solution between pure EG and the stoichiometric ChCl/EG 1:2 DES. The electrochemical behaviors of pure ChCl/EG and EG have been characterized for comparison (Figure S1).

From the electrochemical point of view, the main difference between the two solvents considered, ChCl/EG 1:2 and EG, is the availability of chloride ions. ChCl/EG 1:2, due to the presence of choline chloride, contains a large amount of available Cl^-, which readily forms complexes with most metal ions M^{n+}. Coherently, chloride complexes of the kind MCl^{m-} have been demonstrated to be the dominant species in virtually all DESs[15] where a large excess of Cl^- is present. Pure EG, on the contrary, does not contain Cl^-. The only chloride ions introduced in EG based baths are, eventually, the ones resulting from the metal halides added to provide reducible ions for electrodeposition. In this case, which corresponds to the situation encountered in the present work, an excess of Cl^- is not available and MCl^{m-} species are less prone to form. Knetsch et al. demonstrated, however, that ethylene glycol forms mixed complexes of the kind $M_n(EG)_mCl_p$ with metal halides.[63] Such mixed complexes are characterized by high stability, and they can be easily isolated. Ruttink et al. and Maltanava et al. described the formation of $M_n(EG)_mCl_p$ complexes as well.[50,64] A similar situation may occur also in pure EG based electrolytes, whose environment presents a favorable stoichiometry.

Parts a and b of Figure 2 depict the electrochemical behavior of Zn(II) in ChCl/EG and EG, respectively. The three solutions (ChCl/EG 1:2, ChCl/EG 1:4.5, and pure EG) contained the same amount of zinc salt: 0.2 M $ZnCl_2$. Proper practice imposes, where possible, to evaluate the potential of the redox peaks (E_{peak}) for each electrochemical reaction taking place in an electrolyte. In some cases, however, no clear redox peaks are visible. This is the case of many voltammograms reported in the present work, and for this reason, the reaction onset potential (E_{on}) was evaluated to allow full data comparison. In ChCl/EG 1:2 (Figure 2a), the $Zn^{2+} \rightarrow Zn^0$ reduction (Zn_{red} in the graph) starts around −1.01 V vs Pt and presents a peak around −1.2 V vs Pt. The situation is similar when the ChCl/EG ratio is reduced to 1:4.5 (Figure 2a), with E_{on} for Zn_{red} at −1.02 V vs Pt and E_{peak} around −1.2 V vs Pt. The behavior observed in the case of ChCl/EG 1:2 and 1:4.5 presents important analogies with other existing studies on Zn deposition from DESs.[65,66] Conversely, in EG (Figure 2b), the Zn_{red} reaction starts at −1.11 V vs Pt and does not present a defined peak. This value is slightly lower than the one that was observed in the case of Zn^{2+} reduction in an EG based electrolyte containing zinc acetate.[47] The reason may reside in the different complexation: an acetate containing EG electrolyte does not present chloride moieties, and Zn is consequently forced to form different complexes.[47] In both cases, finally, a broad anodic stripping peak (Zn_{ox}) can be observed.

A similar approach was followed to investigate the behavior of Ni(II) in ChCl/EG and EG (Figure 2c and d). The three solutions (ChCl/EG 1:2, ChCl/EG 1:4.5, and pure EG) contained the same amount of nickel salt: 0.2 M $NiCl_2$. In the case of Ni electroreduction, which is identified by Ni_{red} in the graphs and takes place as $Ni^{2+} \rightarrow Ni^0$, the situation presents important differences between the ChCl/EG and the EG based electrolytes. In ChCl/EG 1:2 (Figure 2c), reduction starts (E_{on}) around −0.52 V vs Pt, which is a value slightly higher than the one (−0.62 V vs Pt) observed in ChCl/EG 1:4.5 (Figure 2c). In analogy with Zn(II) behavior in ChCl/EG 1:2, also Ni(II) presents similarities with the existing literature.[16] The pure EG based electrolyte presents a value of E_{on} for Ni_{red} equal to −0.67 V vs Pt. The observed variation of E_{on} with respect to the ratio between ChCl and EG is indicative of an increasing complexation level when more EG is present in the electrolyte. A reduction peak is visible in the case of ChCl/EG 1:2 around −0.8 V vs Pt, whereas the curve obtained in EG presents a plateau after −0.65 V vs Pt. The presence of such a plateau is indicative of a diffusion-limited reaction. A major difference between the two electrolytes resides in the anodic branch of the voltammetries. For ChCl/EG based electrolytes, an anodic peak (Ni_{ox}) presenting a reduced intensity is visible around 0.2 V vs Pt. Conversely, in the case of EG, a broad anodic stripping peak can be seen, which is indicative of a more favorable anodic reaction kinetic.

Voltammetries were then performed on the complete ZnNi solutions, with either ChCl/EG or EG as solvents (Figure 2e and f). The ChCl/EG based bath contained 0.2 M Zn(II) and 0.13 M Ni(II), while the EG based bath contained 0.2 M Zn(II) and 0.15 M Ni(II). In all of the cases, a neat separation between the two reduction peaks was observed. In ChCl/EG 1:2, Ni reduction (Ni_{red}) started around −0.5 V vs Pt and peaked around −0.8 V vs Pt, while Zn_{red} started at −1.17 V vs Pt. In ChCl/EG 1:4.5, Ni reduction (Ni_{red}) started around −0.55 V vs Pt and peaked around −0.8 V vs Pt, while Zn_{red} started at −1.07 V vs Pt. In pure EG, finally, Ni reduction (Ni_{red}) started around −0.68 V vs Pt, while Zn_{red} started at −1.17 V vs Pt. Different anodic peaks can be observed in the anodic branch of the ZnNi voltammograms. These results from the progressive stripping of Zn and Ni are generically identified as (Zn_{ox}/Ni_{ox}).

Table 1 summarizes all of the data obtained and allows a direct comparison between Zn, Ni, and ZnNi containing electrolytes.

A first important consideration comes from the comparison between E_{on} values in different solvents. E_{on} values present the tendency to increase when the relative concentration of EG in the electrolyte increases. This is probably indicative of a higher level of complexation. When comparing ZnNi electrolytes with the pure metal solutions, it can be observed that Zn and Ni E_{on} values shift. The Ni reduction onset tendentially occurs at more positive potentials, while Zn E_{on} shifts toward more negative values.

Figure S2 describes the effect of varying Zn(II)/Ni(II) relative ratios on the voltammograms. As expectable, curves

https://dx.doi.org/10.1021/acs.jpcb.0c04784
J. Phys. Chem. B 2020, 124, 10739−10751

obtained in ChCl/EG progressively change in intensity when the Zn(II)/Ni(II) ratio varies. This tendency, which is correlated to the variation of the overall quantity of metal salts present in the solution, is evident also in the case of EG based electrolytes.

Potentiostatic ZnNi Electrodeposition. Potentiostatic ZnNi depositions were performed on steel from both ChCl/EG 1:2 and EG based electrolytes. Also, in this case, a ChCl/EG 1:4.5 electrolyte was used together with ChCl/EG 1:2 and EG to investigate an intermediate anions complexation condition. Figure 3 represents the results obtained in terms of composition, determined via X-ray fluorescence spectroscopy (XRF).

For ChCl/EG, the potential was scanned between −0.8 V vs Pt and −1.6 V vs Pt, mapping thus the resulting ZnNi layer composition. It is interesting to notice that, at higher EG contents (ChCl/EG 1:4.5 vs ChCl/EG 1:2), the electrolyte tends to yield higher Ni concentrations (Figure 3a). This appears counterintuitive, since higher EG concentrations decrease E_{on} for Ni_{red} (decreasing thus the ΔE_{on} between Zn_{red} and Ni_{red}). This effect, visible in Table 1, should lead to a decrease in the concentration of the more noble metal, i.e., Ni. It cannot be ignored, however, the fact that ZnNi deposits following an anomalous co-deposition mechanism.[4] Consequently, the effect of complexation can be different with respect to the normal co-deposition mechanism and can affect, besides deposition potentials, also the surface reactions at the base of anomalous co-deposition. Some literature studies[67,68] suggest that, in the case of ZnNi co-deposition in aqueous solutions, a higher complexation level increases Ni content. The trend is further confirmed by looking at Figure 3b, where compositional data obtained from the pure EG ZnNi electrolyte are plotted together with the data from ChCl/EG 1:4.5 and ChCl/EG 1:2. In this case, the potential ranged between −1.2 and −2 V vs Pt. Once again, a significant increase in Ni content was observed moving from ChCl/EG to pure EG (thus increasing the EG content).

Figure 3c depicts the effect of the Zn(II)/Ni(II) ratio on the final layer composition in a ChCl/EG 1:4.5 electrolyte. It is not surprising that, by decreasing the amount of Ni^{2+} in the bath, i.e., increasing the Zn(II)/Ni(II) ratio, the final Ni amount in the layer decreases. The same effect was observed in the case of the EG based electrolyte (Figure 3d).

Anomalous co-deposition is defined as follows: the percentage of the more noble metal in the deposit is lower than the percentage of the same in the electrolyte. This condition can be conveniently represented, in the case of ZnNi co-deposition, in a diagram of the kind % mol. Ni in the electrolyte vs % mol. Ni in the deposit (Figure 3e and f). The black line represents the condition in which the Ni percentage in the bath equals the Ni concentration in the deposited layer. Thus, ZnNi co-deposition can be defined as anomalous when the resulting layer presents a composition that lies below the line. If data reported in Figure 3c and d are plotted as atomic percentages, the result visible in Figure 3e and f is obtained. It appears that ZnNi co-deposition from ChCl/EG 1:4.5 and EG presents an anomalous character, especially at lower deposition potentials. This effect is related to the anomalous co-deposition mechanism: since Ni deposition is partially inhibited by the Zn deposition reaction, the effect is more evident when the percentage of Zn is higher (at low deposition potentials). Both electrolytes start to show anomalous co-deposition at potentials lower than −1.2 V vs Pt.

Electrodeposited ZnNi Phase Composition. From the phase composition point of view, ZnNi alloys in the 15−26% at. Ni should be totally composed of a cubic γ ZnNi phase.[69] This is only partially true for electrodeposited ZnNi, as already demonstrated in the literature.[70,71] In particular, plated ZnNi typically forms a metastable γ phase, which is characterized by a lower degree of ordering with respect to the equilibrium cubic γ phase. This behavior is a direct consequence of the technique employed to obtain the layer. Electrodeposition, as a matter of fact, is a deposition methodology that often works under nonequilibrium conditions and forms metastable structures[72] characterized by an enthalpy higher than their equilibrium counterparts. In electroplated ZnNi, in particular, such an increased level of enthalpy can be associated with Ni atoms that are randomly distributed in the lattice positions instead of being located in preferential sublattice sites.

Formation of a metastable γ ZnNi phase, originally observed by performing XRD on layers obtained from aqueous solutions,[70,71] is confirmed also in the case of layers plated from nonaqueous electrolytes like ChCl/EG and EG (Figure 4). In particular, parts a and b of Figure 4 report the XRD spectra obtained from a ZnNi layer (20% wt Ni) plated from ChCl/EG 1:2 before and after annealing, respectively. Parts c and d of Figure 4 report the XRD spectra obtained from a ZnNi layer (18% wt Ni) plated from EG before and after annealing, respectively. As-plated ZnNi layers present a characteristic XRD pattern, which does not fully correspond to any equilibrium ZnNi intermetallic. Experimental features match the positions of calculated XRD peaks for a γ structure with Ni atoms randomly distributed over all atomic sites (Table S1), demonstrating thus the presence of a metastable phase also in the case of ZnNi plated from ChCl/EG and EG.

After annealing, layers from both ChCl/EG and EG developed the complete set of γ phase peaks. The new peaks that appeared as a consequence of annealing are evident by comparing Figure 4a and c (before annealing) with Figure 4b and d (after annealing). Such new features, once again, find exact correspondence in the calculated peaks (Table S1). The annealing treatment may promote atomic rearrangement, leading to a more stable structure where Ni atoms occupy the outer tetrahedral sites in the cubic cell. Nevertheless, atomic rearrangement might be incomplete after the annealing run and a fraction of Ni atoms must occupy sublattice sites other than the outer tetrahedral ones. Actually, these sites are fully occupied with a Ni percentage of 14 wt % and the composition of the examined layers is beyond this limit. Therefore, it is not surprising that the diffraction spectrum of the annealed layers is still consistent with the calculated XRD pattern of the random solid solution.

Crystallite size was evaluated for layers obtained from both ChCl/EG and EG employing the well-known Scherrer equation. Two intense peaks (330/411 and 552/633) were employed, and their full width at half-maximum (fwhm) was evaluated. The mean crystallite size for ZnNi from ChCl/EG was found to be 17.4 ± 0.52 nm, while the mean crystallite size for ZnNi from EG was found to be equal to 11.06 ± 1.84 nm. As expected, the crystallite size increased as a consequence of annealing. In particular, it was found to be equal to 37.61 ± 0.16 nm in the case of ChCl/EG and 27.44 ± 3.71 nm in the case of EG.

Some unidentified small peaks are present in Figure 4. Such features, however, are all located at low angles, suggesting the presence of minor quantities of oxides or hydroxides on the

https://dx.doi.org/10.1021/acs.jpcb.0c04784
J. Phys. Chem. B 2020, 124, 10739−10751

surface. No difference in the phase composition was observed between the ZnNi layers deposited from ChCl/EG 1:2, ChCl/EG 1:4.5, or pure EG.

ZnNi Surface Morphology. SEM was employed to morphologically characterize the surface of ZnNi layers deposited from ChCl/EG 1:2, ChCl/EG 1:4.5, and pure EG. Figure 5 depicts the result obtained.

The layer obtained from ChCl/EG 1:2 (Figures 5a and S3; −1.2 V, 0.2 M $ZnCl_2$ + 0.13 M $NiCl_2{\cdot}6H_2O$) showed a relatively coarse morphology (Figure S3), characterized by the presence of irregular nodular structures on the surface (Figure 5a). In the case of ChCl/EG 1:4.5 (Figure 5b; −1.3 V, 0.2 M $ZnCl_2$ + 0.13 M $NiCl_2{\cdot}6H_2O$) and pure EG (Figure 5c and d; −1.8 V, 0.4 M $ZnCl_2$ + 0.05 M $NiCl_2{\cdot}6H_2O$), conversely, the morphology became more fine-grained and uniform. At higher magnification (Figure 5d), the surface of the layer obtained from EG evidenced a uniform distribution of micrometric semiprismatic nodules on the surface. The mean thickness of the samples depicted in figure was between 3 and 4 μm. Some minor cracks are evident in Figure 5a and d, probably as a result of internal stress accumulation in the layer. Such cracks became more evident at increasing layer thickness, as visible in Figure S4 (layer thickness 13 μm).

EDS graphs (Figures S5, S6, and S7) evidenced a negligible chlorine contamination of the layer. This demonstrates that Cl^- ions present in the electrolytes are not actively incorporated in the final coatings. Limited oxygen and carbon contamination was detected. In general, layers obtained from both ChCl/EG and pure EG are characterized by high purity.

ZnNi Corrosion Behavior. The corrosion behavior of the electrodeposited ZnNi coatings was investigated performing linear scan potentiometry tests (Figure 6). Corrosion potentials and currents of ZnNi alloys plated from ChCl/EG 1:2, ChCl/EG 1:4.5, and pure EG were compared with the corrosion properties of uncoated steel in order to estimate their corrosion protection. Moreover, the behavior of a ZnNi layer (14% wt Ni) plated from a commercial aqueous alkaline ZnNi electrolyte (Glovel 800 by GLOMAX) was acquired and used for comparison. Optimal conditions provided by the manufacturer were employed for the deposition of the commercial ZnNi sample.

Tafel extrapolation was used to calculate the corrosion potentials (E_{corr}) and the corrosion current densities (I_{corr}) of ZnNi alloys in 3.5% NaCl. The result obtained is shown visually in Figure 6 and numerically in Table 2.

As expected, the corrosion potential of all ZnNi alloys was more negative if compared to steel (−440 mV vs Ag/AgCl) and slightly higher than zinc (which has corrosion potentials not higher than −1000 mV vs Ag/AgCl in 3.65% wt NaCl solutions[73]) as a consequence of their nickel content. In ZnNi, during corrosion, Zn dissolves preferentially and leaves a layer enriched with Ni. This layer can act as a physical barrier to slow down further corrosion.[74] Despite the formation of this protective layer, the samples did not show evident signs of passivity. This behavior is in accordance with the literature, where ZnNi layers tested in NaCl solution behaved in an analogous way.[75−78]

In general, all of the alloys obtained presented corrosion potentials similar to the commercial ZnNi sample. The maximum E_{corr} difference with respect to the Glovel plated ZnNi layer E_{corr} was 76 mV vs Ag/AgCl toward more negative potentials (obtained from the 20% Ni wt from the ChCl/EG 1:2 sample) and 52 mV vs Ag/AgCl toward more positive potentials (obtained from the 15% Ni wt from the ChCl/EG 1:4.5 sample). By considering the data obtained, it appears that ZnNi alloys deposited from ChCl/EG (both 1:2 and 1:4.5) present corrosion currents lower than commercial ZnNi, which slightly depend on Ni content. ZnNi plated from EG, conversely, showed corrosion currents comparable to commercial Glovel ZnNi.

CONCLUSIONS

Choline chloride/ethylene glycol and pure ethylene glycol were successfully employed as non-aqueous solvents for ZnNi deposition. From the electrochemical point of view, both Zn(II) and Ni(II) showed a complexation level dependent on the relative ratio between ChCl and EG. In particular, the separation between reduction onset potentials decreased by increasing EG concentration. This is indicative of a stronger complexation, which can be explained with the possible disappearance of MCl^{m-} complexes in favor of $M_n(EG)_mCl_p$ mixed EG−chloride moieties. ZnNi electrodeposition was demonstrated to follow, analogously to aqueous solutions, an anomalous co-deposition mechanism. Potentiostatic deposition tests evidenced an anomalous behavior especially at potentials lower than −1.2 V vs Pt, where Zn co-deposited preferentially. For all of the electrolytes studied, it was possible to obtain a composition range between 10 and 20% wt, which is the most interesting for corrosion protection applications. ZnNi layers were found to be free from substantial contamination. The phase composition of ZnNi coatings plated from both ChCl/EG and EG was studied via XRD. As-plated layers were all characterized by the presence of a metastable ZnNi γ phase, similarly to layers obtained from aqueous solutions. A good corrosion resistance, equivalent or better with respect to the commercial ZnNi layer, was observed during potentiodynamic polarization tests. Corrosion currents ranged between 1.6 and 18.1 $\mu A/cm^2$, with a value of 11.8 $\mu A/cm^2$ for commercial ZnNi. Corrosion potentials were found to vary between −902 and −774 mV vs Ag/AgCl, with a value of −826 mV vs Ag/AgCl for commercial ZnNi. Corrosion properties were found to vary, as expected, as a result of the solution employed to deposit the layer. In conclusion, the results obtained justify the interest in nonaqueous electrolytes for ZnNi deposition.

ASSOCIATED CONTENT

Supporting Information

The Supporting Information is available free of charge at https://pubs.acs.org/doi/10.1021/acs.jpcb.0c04784.

Voltammetries of pure ChCl/EG 1:2, pure ChCl/EG 1:4.5, and pure EG; voltammetries of ZnNi electrolytes with different Zn(II)/Ni(II) ratios; calculated XRD peaks for a ZnNi γ phase containing randomly placed Ni atoms; SEM images of ZnNi layers plated from ChCl/EG 1:2, ChCl/EG 1:4.5, and EG; and EDS analysis of ZnNi layers plated from ChCl/EG 1:2, ChCl/EG 1:4.5, and EG (PDF)

AUTHOR INFORMATION

Corresponding Author

L. Magagnin − *Dipartimento di Chimica, Materiali e Ingegneria Chimica Giulio Natta, 20131 Milano, Italy;* orcid.org/0000-0001-5553-6441; Email: luca.magagnin@polimi.it

https://dx.doi.org/10.1021/acs.jpcb.0c04784
J. Phys. Chem. B 2020, 124, 10739−10751

Authors

R. Bernasconi − *Dipartimento di Chimica, Materiali e Ingegneria Chimica Giulio Natta, 20131 Milano, Italy;* orcid.org/0000-0003-2193-8017

G. Panzeri − *Dipartimento di Chimica, Materiali e Ingegneria Chimica Giulio Natta, 20131 Milano, Italy*

G. Firtin − *Dipartimento di Chimica, Materiali e Ingegneria Chimica Giulio Natta, 20131 Milano, Italy*

B. Kahyaoglu − *Dipartimento di Chimica, Materiali e Ingegneria Chimica Giulio Natta, 20131 Milano, Italy*

L. Nobili − *Dipartimento di Chimica, Materiali e Ingegneria Chimica Giulio Natta, 20131 Milano, Italy*

Complete contact information is available at: https://pubs.acs.org/10.1021/acs.jpcb.0c04784

Notes

The authors declare no competing financial interest.

■ ACKNOWLEDGMENTS

The authors received no financial support for the research, authorship, or publication of the present work.

■ REFERENCES

(1) Fratesi, R.; Roventi, G. Corrosion Resistance of Zn-Ni Alloy Coatings in Industrial Production. *Surf. Coat. Technol.* **1996**, *82* (1−2), 158−164.

(2) Fashu, S.; Khan, R. Recent Work on Electrochemical Deposition of Zn-Ni (-X) Alloys for Corrosion Protection of Steel. *Anti-Corros. Methods Mater.* **2019**, *66* (1), 45−60.

(3) Roventi, G.; Fratesi, R.; Della Guardia, R. A.; Barucca, G. Normal and Anomalous codeposition of Zn-Ni Alloys from Chloride Bath. *J. Appl. Electrochem.* **2000**, *30* (2), 173−179.

(4) Brenner, A. Electrodeposition of Alloys: PRINCIPLES and PRACTICE. *Electrodepos. Alloy.* **1963**, No. ii.

(5) Zech, N. *Anomalous Codeposition of Iron Group Metals: II. Mathematical Model* **1999**, *146*, 2892.

(6) Kwon, M.; Jo, D.-h.; Cho, S. H.; Kim, H. T.; Park, J.-T.; Park, J. M. Characterization of the Influence of Ni Content on the Corrosion Resistance of Electrodeposited Zn-Ni Alloy Coatings. *Surf. Coat. Technol.* **2016**, *288*, 163−170.

(7) Yang, H. Y.; Guo, X. W.; Chen, X. B.; Wang, S. H.; Wu, G. H.; Ding, W. J.; Birbilis, N. On the Electrodeposition of Nickel-Zinc Alloys from a Eutectic-Based Ionic Liquid. *Electrochim. Acta* **2012**, *63*, 131−138.

(8) Pereira, N. M.; Pereira, C. M.; Araújo, J. P.; Silva, A. F. Influence of Amines on the Electrodeposition of Zn-Ni Alloy from a Eutectic-Type Ionic Liquid. *J. Electrochem. Soc.* **2015**, *162* (8), D325−D330.

(9) Fashu, S.; Gu, C. D.; Wang, X. L.; Tu, J. P. Influence of Electrodeposition Conditions on the Microstructure and Corrosion Resistance of Zn-Ni Alloy Coatings from a Deep Eutectic Solvent. *Surf. Coat. Technol.* **2014**, *242*, 34−41.

(10) Fashu, S.; Gu, C. D.; Zhang, J. L.; Huang, M. L.; Wang, X. L.; Tu, J. P. Effect of EDTA and NH4Cl Additives on Electrodeposition of Zn-Ni Films from Choline Chloride-Based Ionic Liquid. *Trans. Nonferrous Met. Soc. China* **2015**, *25* (6), 2054−2064.

(11) Li, R.; Dong, Q.; Xia, J.; Luo, C.; Sheng, L.; Cheng, F.; Liang, J. Electrodeposition of Composition Controllable Zn−Ni Coating from Water Modified Deep Eutectic Solvent. *Surf. Coat. Technol.* **2019**, *366*, 138−145.

(12) Abbott, A. P.; Boothby, D.; Capper, G.; Davies, D. L.; Rasheed, R. K. Deep Eutectic Solvents Formed between Choline Chloride and Carboxylic Acids: Versatile Alternatives to Ionic Liquids. *J. Am. Chem. Soc.* **2004**, *126* (29), 9142−9147.

(13) Abbott, A. P.; McKenzie, K. J. Application of Ionic Liquids to the Electrodeposition of Metals. *Phys. Chem. Chem. Phys.* **2006**, *8*, 4265−4279.

(14) Bernasconi, R.; Panzeri, G.; Accogli, A.; Liberale, F.; Nobili, L.; Magagnin, L. Electrodeposition from Deep Eutectic Solvents. In *Progress and Developments in Ionic Liquids*; InTech, 2017.

(15) Smith, E. L.; Abbott, A. P.; Ryder, K. S. Deep Eutectic Solvents (DESs) and Their Applications. *Chem. Rev.* **2014**, *114* (21), 11060−11082.

(16) Abbott, A. P.; Ballantyne, A.; Harris, R. C.; Juma, J. A.; Ryder, K. S. A Comparative Study of Nickel Electrodeposition Using Deep Eutectic Solvents and Aqueous Solutions. *Electrochim. Acta* **2015**, *176*, 718−726.

(17) Smith, E. L. Deep Eutectic Solvents (DESs) and the Metal Finishing Industry: Where Are They Now? *Trans. Inst. Met. Finish.* **2013**, *91* (5), 241−248.

(18) Huynh, T. C.; Dao, Q. P. D.; Truong, T.-N.; Doan, N.-G.; Ho, S.-L. Electrodeposition of Aluminum on Cathodes in Ionic Liquid Based Choline Chloride/Urea/ALCL3. *Environ. Pollut.* 2014 3 (4). DOI: 10.5539/ep.v3n4p59.

(19) Bernasconi, R.; Magagnin, L. Electrodeposition of Nickel from DES on Aluminium for Corrosion Protection. *Surf. Eng.* **2017**, *33* (2), 131−135.

(20) Smith, E. L.; Fullarton, C.; Harris, R. C.; Saleem, S.; Abbott, A. P.; Ryder, K. S. Metal Finishing with Ionic Liquids: Scale-up and Pilot Plants from IONMET Consortium. *Trans. Inst. Met. Finish.* **2010**, *88* (6), 285−291.

(21) Ferreira, E. S. C.; Pereira, C. M.; Silva, A. F. Electrochemical Studies of Metallic Chromium Electrodeposition from a Cr(III) Bath. *J. Electroanal. Chem.* **2013**, *707*, 52−58.

(22) Abbott, A. P.; Capper, G.; Davies, D. L.; Rasheed, R. K. Ionic Liquid Analogues Formed from Hydrated Metal Salts. *Chem. - Eur. J.* **2004**, *10* (15), 3769−3774.

(23) Rahman, M. F.; Bernasconi, R.; Magagnin, L. Electrodeposition of Indium from a Deep Eutectic Solvent. *J. Optoelectron. Adv. Mater.* **2015**, *17* (1−2), 122−126.

(24) Bernasconi, R.; Lucotti, A.; Nobili, L.; Magagnin, L. Ruthenium Electrodeposition from Deep Eutectic Solvents. *J. Electrochem. Soc.* **2018**, *165* (13), D620−D627.

(25) Abbott, A. P.; Barron, J. C.; Ryder, K. S. Electrolytic Deposition of Zn Coatings from Ionic Liquids Based on Choline Chloride. *Trans. Inst. Met. Finish.* **2009**, *87* (4), 201−207.

(26) Whitehead, A. H.; Pölzler, M.; Gollas, B. Zinc Electrodeposition from a Deep Eutectic System Containing Choline Chloride and Ethylene Glycol. *J. Electrochem. Soc.* **2010**, *157* (6), D328.

(27) Abbott, A. P.; Barron, J. C.; Frisch, G.; Ryder, K. S.; Silva, A. F. The Effect of Additives on Zinc Electrodeposition from Deep Eutectic Solvents. *Electrochim. Acta* **2011**, *56* (14), 5272−5279.

(28) Vieira, L.; Whitehead, A. H.; Gollas, B. Mechanistic Studies of Zinc Electrodeposition from Deep Eutectic Electrolytes. *J. Electrochem. Soc.* **2014**, *161* (1), D7−D13.

(29) Yang, H.; Reddy, R. G. Electrochemical Deposition of Zinc from Zinc Oxide in 2:1 Urea/Choline Chloride Ionic Liquid. *Electrochim. Acta* **2014**, *147*, 513−519.

(30) Starykevich, M.; Salak, A. N.; Ivanou, D. K.; Lisenkov, A. D.; Zheludkevich, M. L.; Ferreira, M. G. S. Electrochemical Deposition of Zinc from Deep Eutectic Solvent on Barrier Alumina Layers. *Electrochim. Acta* **2015**, *170*, 284−291.

(31) Ibrahim, S.; Bakkar, A.; Ahmed, E.; Selim, A. Effect of Additives and Current Mode on Zinc Electrodeposition from Deep Eutectic Ionic Liquids. *Electrochim. Acta* **2016**, *191*, 724−732.

(32) Abbott, A. P.; Capper, G.; McKenzie, K. J.; Ryder, K. S. Electrodeposition of Zinc-Tin Alloys from Deep Eutectic Solvents Based on Choline Chloride. *J. Electroanal. Chem.* **2007**, *599* (2), 288−294.

(33) Pereira, N. M.; Salomé, S.; Pereira, C. M.; Silva, A. F. Zn-Sn Electrodeposition from Deep Eutectic Solvents Containing EDTA, HEDTA, and Idranal VII. *J. Appl. Electrochem.* **2012**, *42* (8), 561−571.

(34) Xie, X.; Zou, X.; Lu, X.; Xu, Q.; Lu, C.; Chen, C.; Zhou, Z. Electrodeposition Behavior and Characterization of Copper−Zinc

Alloy in Deep Eutectic Solvent. *J. Appl. Electrochem.* **2017**, *47* (6), 679−689.
(35) Xie, X.; Zou, X.; Lu, X.; Lu, C.; Cheng, H.; Xu, Q.; Zhou, Z. Electrodeposition of Zn and Cu-Zn Alloy from ZnO/CuO Precursors in Deep Eutectic Solvent. *Appl. Surf. Sci.* **2016**, *385*, 481−489.
(36) Fashu, S.; Gu, C. D.; Zhang, J. L.; Zheng, H.; Wang, X. L.; Tu, J. P. Electrodeposition, Morphology, Composition, and Corrosion Performance of Zn-Mn Coatings from a Deep Eutectic Solvent. *J. Mater. Eng. Perform.* **2015**, *24* (1), 434−444.
(37) Bučko, M.; Culliton, D.; Betts, A. J.; Bajat, J. B. The Electrochemical Deposition of Zn−Mn Coating from Choline Chloride−Urea Deep Eutectic Solvent. *Trans. Inst. Met. Finish.* **2017**, *95* (1), 60−64.
(38) Maniam, K. K.; Paul, S. Progress in Electrodeposition of Zinc and Zinc Nickel Alloys Using Ionic Liquids. *Appl. Sci.* **2020**, *10* (15), 5321.
(39) Badea, M. L. M.; Cojocaru, A.; Anicai, L. Electrode Processes in Ionic Liquid Solvents as Mixtures of Choline Chloride with Urea, Ethylene Glycol or Malonic Acid. *UPB Sci. Bull. Ser. B* **2014**, *76* (3), 21−32.
(40) Gabe, D. R. The Role of Hydrogen in Metal Electrodeposition Processes. *J. Appl. Electrochem.* **1997**, *27* (8), 908−915.
(41) Carr, M. J.; Robinson, M. J. The Effects of Zinc Alloy Electroplating on the Hydrogen Embrittlement of High Strength Steels. *Trans. Inst. Met. Finish.* **1995**, *73* (2), 58−64.
(42) Sriraman, K. R.; Brahimi, S.; Szpunar, J. A.; Yue, S. Hydrogen Embrittlement of Zn-, Zn-Ni-, and Cd-Coated High Strength Steel. *J. Appl. Electrochem.* **2013**, *43* (4), 441−451.
(43) Shamsuri, A. A.; Abdullah, D. K. Ionic Liquids: Preparations and Limitations. *Makara J. Sci.* **2011**, *14*, 101−106.
(44) Panzeri, G.; Tresoldi, M.; Nobili, L.; Magagnin, L. Electrodeposition of ZnNi Alloys from Ethylene Glycol/Choline Chloride Based Ionic Liquid. *ECS Trans.* **2016**, *75* (15), 627.
(45) Wu, M.; Nguyen, H. P.; Vullers, R. J. M.; Vereecken, P. M.; Binnemans, K.; Fransaer, J. Electrodeposition of Bismuth Telluride Thermoelectric Films from Chloride-Free Ethylene Glycol Solutions. *J. Electrochem. Soc.* **2013**, *160* (4), D196−D201.
(46) Wu, M.; Binnemans, K.; Fransaer, J. Electrodeposition of Antimony from Chloride-Free Ethylene Glycol Solutions and Fabrication of Thermoelectric Bi2Te3/(Bi1-XSbx)2Te3Multilayers Using Pulsed Potential Electrodeposition. *Electrochim. Acta* **2014**, *147*, 451−459.
(47) Panzeri, G.; Muller, D.; Accogli, A.; Gibertini, E.; Mauri, E.; Rossi, F.; Nobili, L.; Magagnin, L. Zinc Electrodeposition from a Chloride-Free Non-Aqueous Solution Based on Ethylene Glycol and Acetate Salts. *Electrochim. Acta* **2019**, *296*, 465−472.
(48) Panzeri, G.; Accogli, A.; Gibertini, E.; Varotto, S.; Rinaldi, C.; Nobili, L.; Magagnin, L. Electrodeposition of Cobalt Thin Films and Nanowires from Ethylene Glycol-Based Solution. *Electrochem. Commun.* **2019**, *103*, 31−36.
(49) Vorobyova, T. N.; Vrublevskaya, O. N. Electrochemical Deposition of Gold-Tin Alloy from Ethylene Glycol Electrolyte. *Surf. Coat. Technol.* **2010**, *204* (8), 1314−1318.
(50) Maltanava, H. M.; Vorobyova, T. N.; Vrublevskaya, O. N. Electrodeposition of Tin Coatings from Ethylene Glycol and Propylene Glycol Electrolytes. *Surf. Coat. Technol.* **2014**, *254*, 388−397.
(51) Pallaro, M.; Moretto, F. L.; Panzeri, G.; Magagnin, L. Sn-Cu Codeposition from a Non-Aqueous Solution Based on Ethylene Glycol for Wafer-Bonding Applications: Direct and Pulse Electroplating. *Trans. Inst. Met. Finish.* **2018**, *96* (5), 265−268.
(52) Neuróhr, K.; Pogány, L.; Tóth, B. G.; Révész, Á.; Bakonyi, I.; Péter, L. Electrodeposition of Ni from Various Non-Aqueous Media: The Case of Alcoholic Solutions. *J. Electrochem. Soc.* **2015**, *162* (7), D256−D264.
(53) Panzeri, G.; Accogli, A.; Gibertini, E.; Rinaldi, C.; Nobili, L.; Magagnin, L. Electrodeposition of High-Purity Nanostructured Iron Films from Fe(II) and Fe(III) Non-Aqueous Solutions Based on Ethylene Glycol. *Electrochim. Acta* **2018**, *271*, 576−581.
(54) Panzeri, G.; Tresoldi, M.; Rinaldi, C.; Magagnin, L. Electrodeposition of Magnetic SmCo Films from Deep Eutectic Solvents and Choline Chloride-Ethylene Glycol Mixtures. *J. Electrochem. Soc.* **2017**, *164* (13), D930−D933.
(55) Lukaczynska, M.; Mernissi Cherigui, E. A.; Ceglia, A.; Van Den Bergh, K.; De Strycker, J.; Terryn, H.; Ustarroz, J. Influence of Water Content and Applied Potential on the Electrodeposition of Ni Coatings from Deep Eutectic Solvents. *Electrochim. Acta* **2019**, *319*, 690−704.
(56) Valverde, P. E.; Green, T. A.; Roy, S. Effect of Water on the Electrodeposition of Copper from a Deep Eutectic Solvent. *J. Appl. Electrochem.* **2020**, *50* (6), 699−712.
(57) Du, C.; Zhao, B.; Chen, X. B.; Birbilis, N.; Yang, H. Effect of Water Presence on Choline Chloride-2urea Ionic Liquid and Coating Platings from the Hydrated Ionic Liquid. *Sci. Rep.* **2016**, *6* (July), 1−14.
(58) Troter, D. Z.; Todorović, Z. B.; Đokić-Stojanović, D. R.; Đorđević, B. S.; Todorović, V.; Konstantinović, S. S.; Veljković, V. B. The Physicochemical and Thermodynamic Properties of the Choline Chloride-Based Deep Eutectic Solvents. *J. Serb. Chem. Soc.* **2017**, *82* (9), 1039−1052.
(59) Abbott, A. P.; Harris, R. C.; Ryder, K. S. Application of Hole Theory to Define Ionic Liquids by Their Transport Properties. *J. Phys. Chem. B* **2007**, *111* (18), 4910−4913.
(60) Reade, G.; Ottewill, G.; Walsh, F. Understanding Electrical and Electrolytic Conductivity. *Trans. Inst. Met. Finish.* **2000**, *78* (2), 89−92.
(61) Mahapatro, A.; Suggu, S. K. Modeling and Simulation of Electrodeposition: Effect of Electrolyte Current Density and Conductivity on Electroplating Thickness. *Adv. Mater. Sci.* **2018**, *3* (2), 1.
(62) Giap, S. G. E. The Hidden Property of Arrhenius-Type Relationship: Viscosity as a Function of Temperature. *J. Phys. Sci.* **2010**, *21* (1), 29−39.
(63) Knetsch, D.; Groeneveld, W. L. Alcohol as Ligands. III. Complexes of Ethylene Glycol with Some Divalent Metal Halides. *Inorg. Chim. Acta* **1973**, *7*, 81−87.
(64) Ruttink, P. J. A.; Dekker, L. J. M.; Luider, T. M.; Burgers, P. C. Complexation of Divalent Metal Ions with Diols in the Presence of Anion Auxiliary Ligands: Zinc-induced Oxidation of Ethylene Glycol to Glycolaldehyde by Consecutive Hydride Ion and Proton Shifts. *J. Mass Spectrom.* **2012**, *47* (7), 869−874.
(65) Alesary, H. F.; Cihangir, S.; Ballantyne, A. D.; Harris, R. C.; Weston, D. P.; Abbott, A. P.; Ryder, K. S. Influence of Additives on the Electrodeposition of Zinc from a Deep Eutectic Solvent. *Electrochim. Acta* **2019**, *304*, 118−130.
(66) Pereira, N. M.; Pereira, C. M.; Araujo, J. P.; Silva, A. F. Zinc Electrodeposition from Deep Eutectic Solvent Containing Organic Additives. *J. Electroanal. Chem.* **2017**, *801*, 545−551.
(67) Rodriguez-Torres, I.; Valentin, G.; Lapicque, F. Electrodeposition of Zinc−Nickel Alloys from Ammonia-Containing Baths. *J. Appl. Electrochem.* **1999**, *29* (9), 1035−1044.
(68) Harris, T. M.; Clair, J. S. Testing the Role of Metal Hydrolysis in the Anomalous Electrodeposition of Ni-Fe Alloys. *J. Electrochem. Soc.* **1996**, *143* (12), 3918.
(69) Okamoto, H. Ni-Zn (Nickel-Zinc). *J. Phase Equilib. Diffus.* **2013**, *34* (2), 153.
(70) Magagnin, L.; Nobili, L.; Cavallotti, P. L. Metastable Zinc−Nickel Alloys Deposited from an Alkaline Electrolyte. *J. Alloys Compd.* **2014**, *615*, S444−S447.
(71) Ieffa, S.; Bernasconi, R.; Nobili, L.; Cavallotti, P. L.; Magagnin, L. Direct and Pulse Plating of Metastable Zn−Ni Alloys. *Trans. Inst. Met. Finish.* **2014**, *92* (6), 321−324.
(72) Povetkin, V. V.; Devyatkova, O. V. Formation of Metastable Phases in the Process of Electrodeposition of Metals and Alloys. *Trans. Inst. Met. Finish.* **1996**, *74* (5), 177−178.
(73) Fayomi, O. S. An Investigation of the Properties of Zn Coated Mild Steel. *Int. J. Electrochem. Sci.* **2012**, *7*, 6555−6570.

https://dx.doi.org/10.1021/acs.jpcb.0c04784
J. Phys. Chem. B 2020, 124, 10739−10751

(74) Hammami, O.; Dhouibi, L.; Triki, E. Influence of Zn−Ni Alloy Electrodeposition Techniques on the Coating Corrosion Behaviour in Chloride Solution. *Surf. Coat. Technol.* **2009**, *203* (19), 2863−2870.
(75) Mosavat, S. H.; Shariat, M. H.; Bahrololoom, M. E. Study of Corrosion Performance of Electrodeposited Nanocrystalline Zn-Ni Alloy Coatings. *Corros. Sci.* **2012**, *59*, 81−87.
(76) Sriraman, K. R.; Brahimi, S.; Szpunar, J. A.; Osborne, J. H.; Yue, S. Characterization of Corrosion Resistance of Electrodeposited Zn-Ni Zn and Cd Coatings. *Electrochim. Acta* **2013**, *105*, 314−323.
(77) Tafreshi, M.; Allahkaram, S. R.; Farhangi, H. Comparative Study on Structure, Corrosion Properties and Tribological Behavior of Pure Zn and Different Zn-Ni Alloy Coatings. *Mater. Chem. Phys.* **2016**, *183*, 263−272.
(78) Rashmi, S.; Elias, L.; Hegde, A. C. Multilayered Zn-Ni Alloy Coatings for Better Corrosion Protection of Mild Steel. *Eng. Sci. Technol. an Int. J.* **2017**, *20* (3), 1227−1232.

https://dx.doi.org/10.1021/acs.jpcb.0c04784
J. Phys. Chem. B 2020, 124, 10739−10751